Arab J. Nucl. Sci. Appl., Vol. 57, 1, 41-50 (2024)

ISSN 1110-0451

Arab Journal of Nuclear Sciences and Applications

Web site: ajnsa.journals.ekb.eg

(E S N S A)

Correlation Influence and Quantification of Grain Size on Radon Radioactivity for (Ca_2SiO_4) Ore Rocks

A. Abdelrazek[1] and M. Mitwalli[1,2]*

[(1)] *Physics Department, Faculty of Science, Mansoura University, Mansoura 35516, Egypt*
[(2)] *National Network for Nuclear Science, Academy of Scientific Research and Technology, Cairo 11334, Egypt*

ARTICLE INFO

Article history:
Received: 13th July 2023
Accepted: 3rd Sept. 2023
Available online: 7th Oct. 2023

Keywords:
Grain Size;
SSNTDs,
Radon,
Ca_2SiO_4,
Radiological Impact,
Environmental Radioactivity.

ABSTRACT

The present study is carried out to investigate the influence of grain size on the level of radon radioactivity for calcium silicate (Ca_2SiO_4) ore rocks, which are used widely in many construction materials, particularly cement. The polymeric nuclear detector is used to determine radon activity concentration and assessment of the radiological impact of (Ca_2SiO_4) ore rocks. In addition to explaining the influence and quantification of grain size on radon radioactivity hence acts as a great radiological impact assessment and radiation protection to specify if it poses a risk to human health, moreover environmental safety. The investigated samples were analyzed by alpha trace detector (LR-115 NTD) to measure the radioactivity concentration of radon, which is produced in the continental crust by the natural decay series of uranium-238 and penetrates the pore spaces where it is imparted by diffusion and sent out into the atmosphere. The research results explained the correlation of grain size which influences the radon exhalation rate. The study indicated a normal radiation level (>1000 Bqm^{-3}) regarding the international limitation and permissible levels recommended by IAEA, ICRP, and UNSCEAR.

1. INTRODUCTION

Nuclear decay is a physical process that occurs off-hand, in a stochastic manner, when atomic nuclei of an isotope undergo internal processes to reach a more stable energy state. Radioactivity is the macroscopic representation of nuclear decay. The process of decay is attributed to the effect of nuclear particles or photon emissions, which carry the surplus energy. Because nuclear radiation can occur in a variety of kinds, abundances, and energy that are unique to each radionuclide, radioactivity analysis is a sophisticated process aimed at identifying and quantifying radioactive isotopes [1]. Relying on the geographical and geological aspects of the environment, naturally occurring radionuclide deposits in the sediments and rocks [2]. Calcium silicates are used in many industries stuff and building materials are their common applications, especially cement and glass. Also, Calcium silicates are extensively involved in the accessory materials and finishes of dwellings such as bricks, and tiles. In addition, it is a supplement material in paper and some plastics manufacturers [3-5]. Furthermore, it's also used in some medical applications as a dental filler application [6, 7] Solid state nuclear track detectors are widely functional in experimental nuclear and particle measurements to detect the charged particles and radiation dosimetry [8, 9]. The benefits of NTDs are their low cost, accuracy, and facilitated setup. There are numerous types of SSNTDs have been enabled to measure radon radioactivity concentration. The cultivated NTD has a distinctive resolution of charged particles [1, 10-13]. Numerous literature studies accomplished to explore the encompasses of some physical and chemical factors, for example, bulk etching and optical properties of the NTDs [8, 14-16]. Passive techniques NTDs are used widely for measuring the ^{222}Rn radioactivity concentration in sediment and rock samples [17]. ^{226}Ra is the product of the ^{238}U series which decays by alpha-emitting into ^{222}Rn radionuclide. This new daughter is mischievous to people's health as a result of the ionization energy of alpha particles [18-24]. Current work aims to determine ^{222}Rn activity concentration and, studies the influence of physical

Corresponding author: meto_mms@yahoo.com
DOI: 10.21608/AJNSA.2023.222779.1764

parameters on ^{222}Rn exhalation rate using LR-115 NTD for traditional Ca_2SiO_4 rocks which are used in construction and building material in Egypt.

2. MATERIALS AND ANALYSIS

2.1. Sampling and Preparation

The Wadi Feiran–Solaf metamorphic complex constitutes an elongated folded belt in southern Sinai, Egypt, that is about 40 km long and 5–11 km wide, trending NW–SE parallel to the orientation of the Najd fault system as shown in Fig. (1). It has evolved and was exhumed in close connection with the activity of this shear zone system [25, 26]. Calcium silicate rocks were gathered from ore quarries in the Sinai Peninsula, and their most notable use is in building materials such as some forms of pottery, glass, and cement of all types. The chemical composition of investigated samples was measured by using X-ray fluorescence analysis (XRF) and Table (1) gives the oxide content of detected elements. The collected rock samples were dehydrated for 60 min. at 110 °C in the electric oven and Table (2) shows the strategy of preparation samples which followed the sequence geological methodology and specifies technical requirements and corresponding test methods for test sieves and International Organization for Standardization (ISO) 3310-1:2016 to obtain target size domain, which applies aperture grain (500 µm down to 0.001 µm), ISO 565. [27, 28]. After the sieving process, each sample was stored for 28 days with the selfsame volume (471.23 cm^3 ± 5%) in the closed stainless-steel cans, and detectors fixed perpendicularly to the sample surface with 11 cm free space as shown in Fig. (2).

Table (1): Chemical composition of the investigated samples from XRF analysis

Oxide	CaO	Na_2O	MgO	Cl	SiO_2	K_2O	SO_3	Fe_2O_3	Al_2O_3
wt%	63.51	0.043	0.24	0.023	0.05	0.007	0.022	0.019	0.017

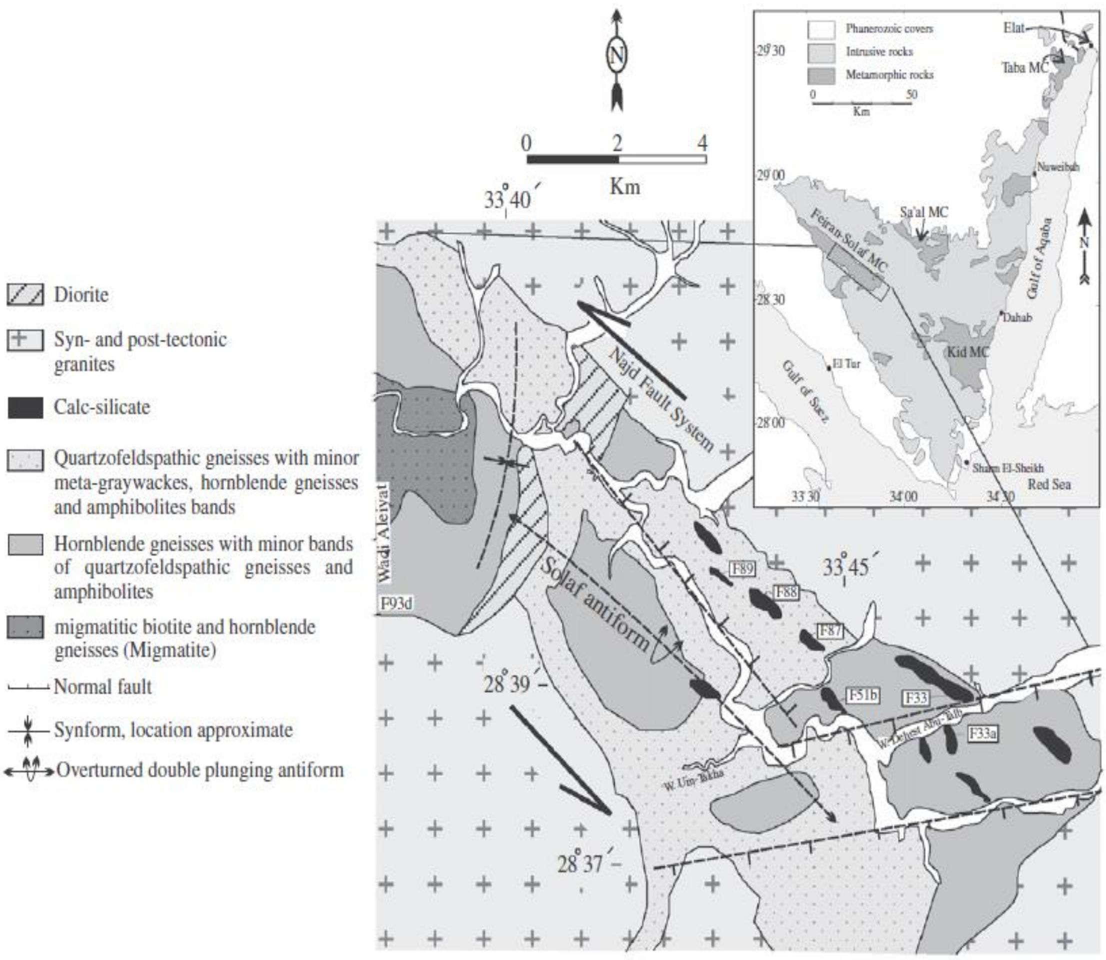

Fig. (1): Location and geological map of investigated area [25, 26]

Table (2): The sampling strategy and domain of investigated samples

No.	Domain	Standardization diameter (μm)	Experimental diameter (μm)	Geometric status
1	D1	5.00E+08	bulk	bulk scale
2	D2	4.00E+08	S ≤ 500	large pebble
3	D3	3.00E+08	400 ≤ S < 500	medium pebble
4	D4	2.00E+08	300 ≤ S < 400	small pebble
5	D5	1.00E+08	200 ≤ S < 300	fine pebble
6	D6	5.00E+07	100 ≤ S < 200	very fin pebble
7	D7	2.50E+07	0.50 ≤ S < 100	sand
8	D8	1.25E+07	0.25 ≤ S < 0.50	fine sand
9	D9	6.25E+06	0.125 ≤ S < 0.25	very fine sand
10	D10	3.13E+06	0.0625 ≤ S < 0.125	1st crushed
11	D11	1.56E+06	0.03125 ≤ S < 0.0625	2nd crushed
12	D12	7.80E+05	0.015625 ≤ S < 0.03125	3rd crushed
13	D13	3.90E+05	0.0078125 ≤ S < 0.015625	1st mashed, powder
14	D14	1.95E+05	0.00390625 ≤ S < 0.0078125	2nd mashed, fine powder
15	D15	9.75E+04	0.001953125 ≤ S < 0.00390625	3rd mashed, absolute powder

2.2. Experimental and Analysis techniques

The solid-state nuclear track detector LR-115 NTD; (type II with thickness 112 μm) was used to measure radon activity concentration. The emulsion sheets of cellulose nitrate carbonate $C_6H_8O_9N_2$ specified with one sensitive face which is very sensitive for any heavy charge particle falling with energy range (1.6 - 4.6) MeV. A texture of LR-115 NTD sheets (1.5 x 1.5 cm) was prepared and fixed at the internal topside to be perpendicular to each sample surface, and the containers were closed firmly as shown in Fig. (2). An emptied closed cans were used to determine the radiation background and all samples were stored for 28 days at a dry and dark place to reach secular equilibrium. The detectors were taken away accurately from the cans and excavated in 100 ml sodium hydroxide solution (10 mg ≅ 2.5 N) within a water bath at 60±1 ^oC for 110 minutes. Then they were taken out from the solution, washed with distilled water for 5 minutes, and then, irradiated sheets placed in 100 ml solution with an equal ratio of water and ethyl alcohol for 5 minutes to stop the interaction and chemical etching process. After that, irradiated LR-115 NTD sheets were washed again with distilled water.

Finally, the LR-115 detectors were dried with fine-drying paper tissue and placed in aluminum sheets. Alpha track counting for each sample was performed by using an optical microscope with a magnification of 640x taking into consideration the background [10, 11, 13, 29].

For the actual summation of alpha tracks, the radiation background was counted and eliminated from the total count of investigated samples [30-32]. Equation (1) gives the radon activity concentration C_{Rn} in Bqm^{-3} at secular equilibrium [10, 11, 13, 29, 33-36]:

$$C_{Rn} = \frac{\rho}{\eta T} \pm \frac{\sqrt{\frac{\alpha}{f\pi r^2}}}{\eta T} \quad (1)$$

where ρ is the density of alpha tracks (tracks/cm^2) and equation (2) was used to calculate the distribution density of alpha tracks [32]:

$$\rho = \frac{\alpha}{f\pi r^2} \pm \sqrt{\frac{\alpha}{f\pi r^2}} \quad (2)$$

where α is the total number of alpha tracks, f is the matrix fields, πr^2 is the fields calibration area, T is the irradiation cycle (28 days), and η is the calibration coefficient of LR-115 [29, 32].

The radon surface exhalation rate E_A was calculated by the equation (3):

$$E_A = \frac{C_{Rn}\, V\, \lambda}{A[T + \frac{1}{\lambda}(e^{-\lambda T} - 1)]} \pm \frac{\sqrt{\frac{\alpha}{f\pi r^2}}\, V\, \lambda}{\eta T A[T + \frac{1}{\lambda}(e^{-\lambda T} - 1)]} \quad \textbf{(3)}$$

where E_A is the radon exhalation rate (Bqm^{-2}h^{-1}), λ is the constant of radon decay (0.00756 h^{-1}), C_{Rn} is the activity concentration of radon (Bqm^{-3}), V is the investigated sample volume (m^3), A is the surface area (m^2), and T is irradiation cycle [37-39].

3. RESULTS AND DISCUSSION

The results of the investigated different domains mentioned in Table (2) indicate that the emission of radon depends on the physical dimension of grain size. The values of track density and radon activity concentration rather than exhalation rate were proportional to the growth in the grain size as shown in Table (3). The values of track density ranged from 129.92 ± 30.62 to 1082.69 ± 81.66 (track/cm^2).

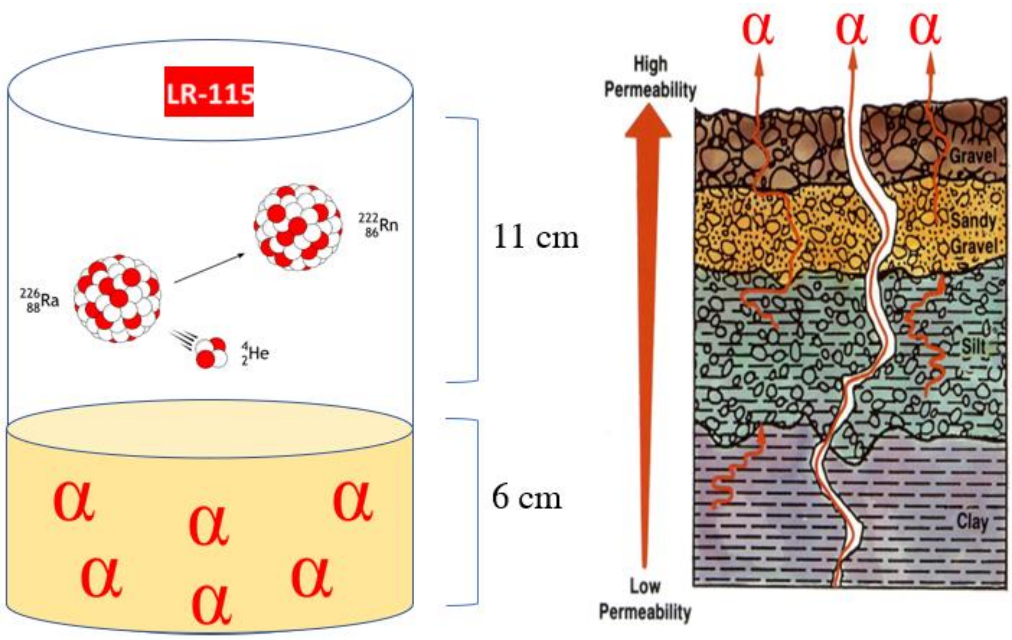

Fig. (2): Set-up system of cans technique used to measure radon activity concentrations

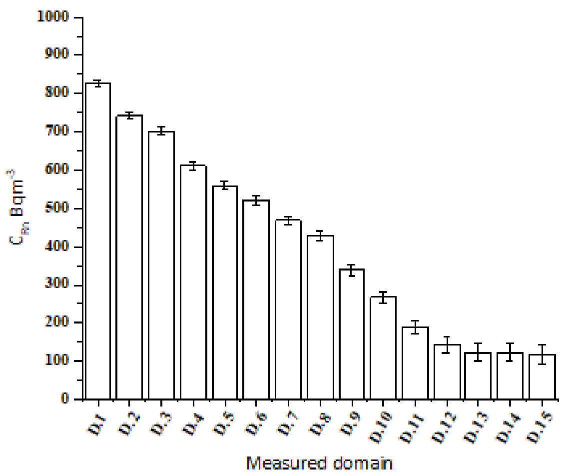

Fig. (3): Comparison of C_{Rn} values into different domain sizes of investigated samples

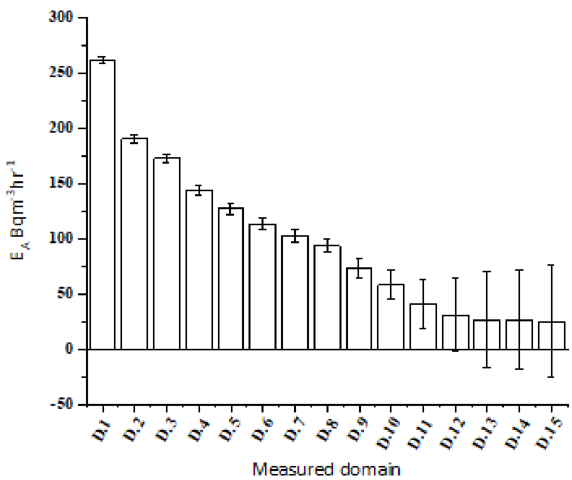

Fig. (4): Comparison of E_A into different domain sizes of investigated samples

The values of ^{222}Rn concentration ranged from 117.05 ± 27.59 to 825.40 ± 73.57 (Bqm^{-3}) and Fig. (3) show the comparison between values of C_{Rn} of different sample domain in addition, the histogram of Fig (5) shows the statistical frequency of three categories of radon concentration based on samples domine. The calculations of surface exhalation rate values ranged from 26.98 ± 11.73 to 261.64 ± 7.19 ($mBqm^{-2}h^{-1}$) which demonstrates the reverse proportion between of physical grain size domain of investigated samples and both of radon concentration and its exhalation rate. Figures (4 and 6) show the comparison between the values of E_A of different sample domains and the statistical frequency, respectively.

Table (3): The values of track density ρ, radon activity concentration C_{Rn}, and exhalation rate E_A of investigated samples

No.	Domain	ρ (Track cm^{-2})	C_{Rn} (Bqm^{-3})	E_A ($mBqm^{-2}h^{-1}$)
1	D1	1082.69 ± 81.66	825.40 ± 73.57	261.64 ± 7.19
2	D2	822.84 ± 77.07	741.30 ± 69.43	190.05 ± 6.88
3	D3	779.53 ± 75.01	702.28 ± 67.58	172.58 ± 6.6
4	D4	678.48 ± 69.98	611.24 ± 63.05	144.20 ± 6.33
5	D5	620.74 ± 66.94	559.23 ± 60.31	126.84 ± 6.09
6	D6	577.43 ± 64.56	520.21 ± 58.16	113.60 ± 5.86
7	D7	519.69 ± 61.25	468.19 ± 55.18	102.24 ± 6.07
8	D8	476.38 ± 58.64	429.17 ± 52.83	93.72 ± 6.07
9	D9	375.33 ± 52.05	338.14 ± 46.89	73.84 ± 6.47
10	D10	295.93 ± 46.22	266.60 ± 41.64	58.22 ± 7.68
11	D11	209.32 ± 38.87	188.58 ± 35.02	41.18 ± 9.10
12	D12	158.79 ± 33.86	143.05 ± 30.50	31.24 ± 10.31
13	D13	137.14 ± 31.46	123.55 ± 28.34	26.98 ± 11.73
14	D14	137.14 ± 31.46	123.55 ± 28.34	26.98 ± 12.13
15	D15	129.92 ± 30.62	117.05 ± 27.59	25.56 ± 12.94

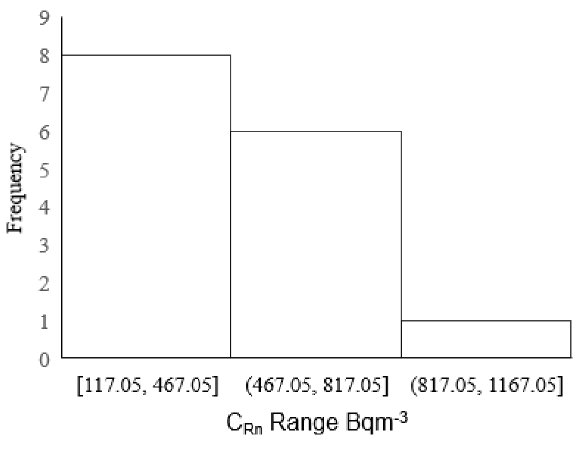

Fig. (5): The histogram of three categories of radon concentration based on sample domine and comparison of its frequency

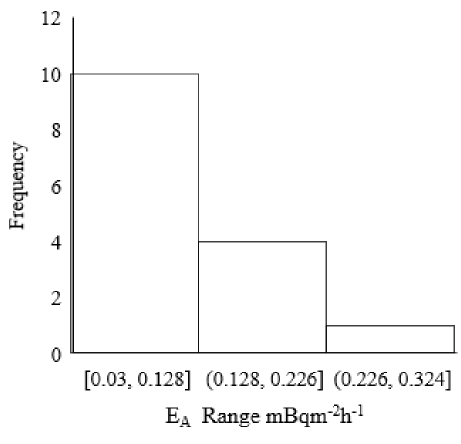

Fig. (6): The histogram of three categories of radon exhalation rate based on sample domine and comparison of its frequency

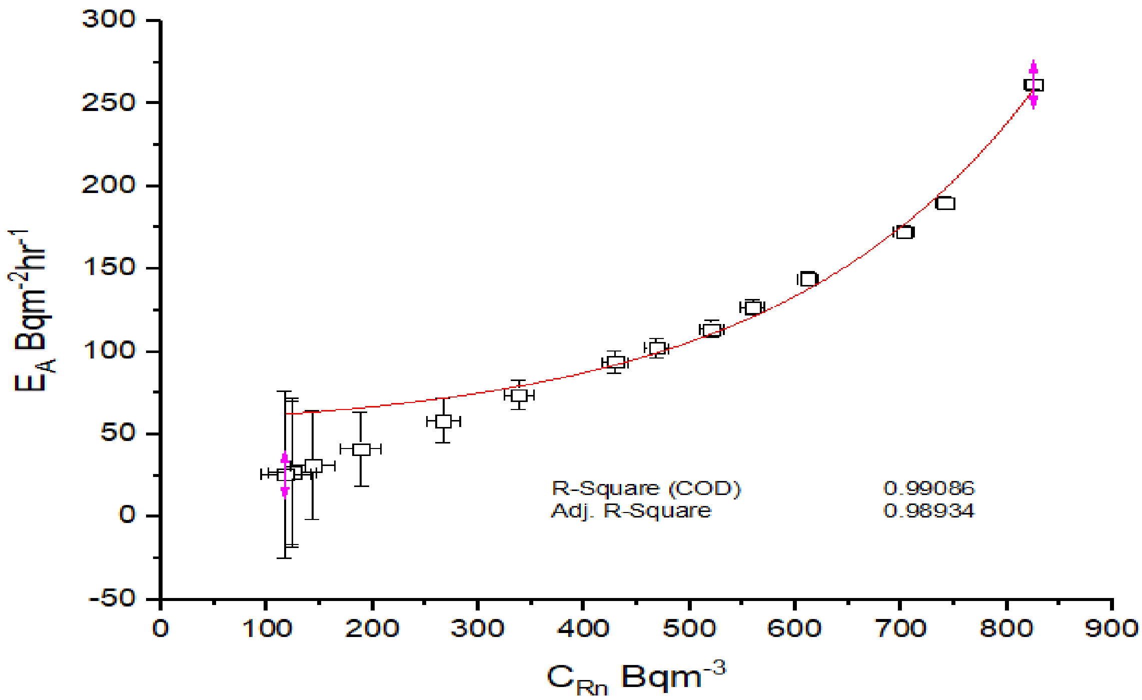

Fig. (7): Exponentially correlation between C_{Rn} and E_A

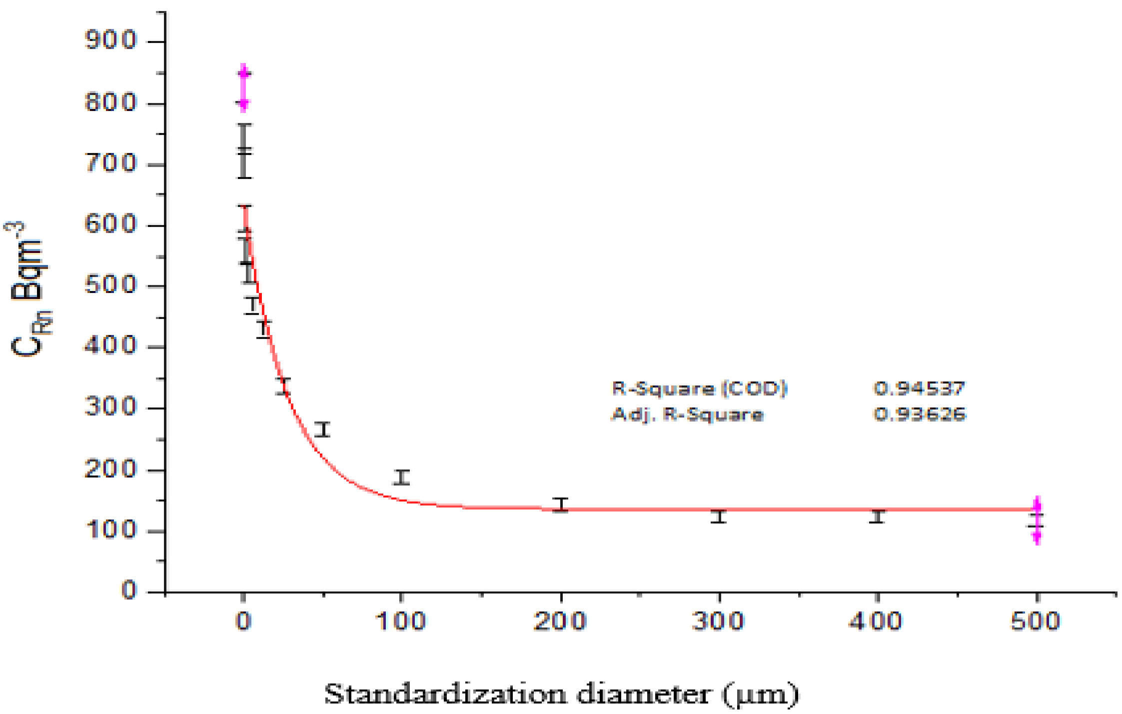

Fig. (8): Exponentially correlation between C_{Rn} and standardization domain

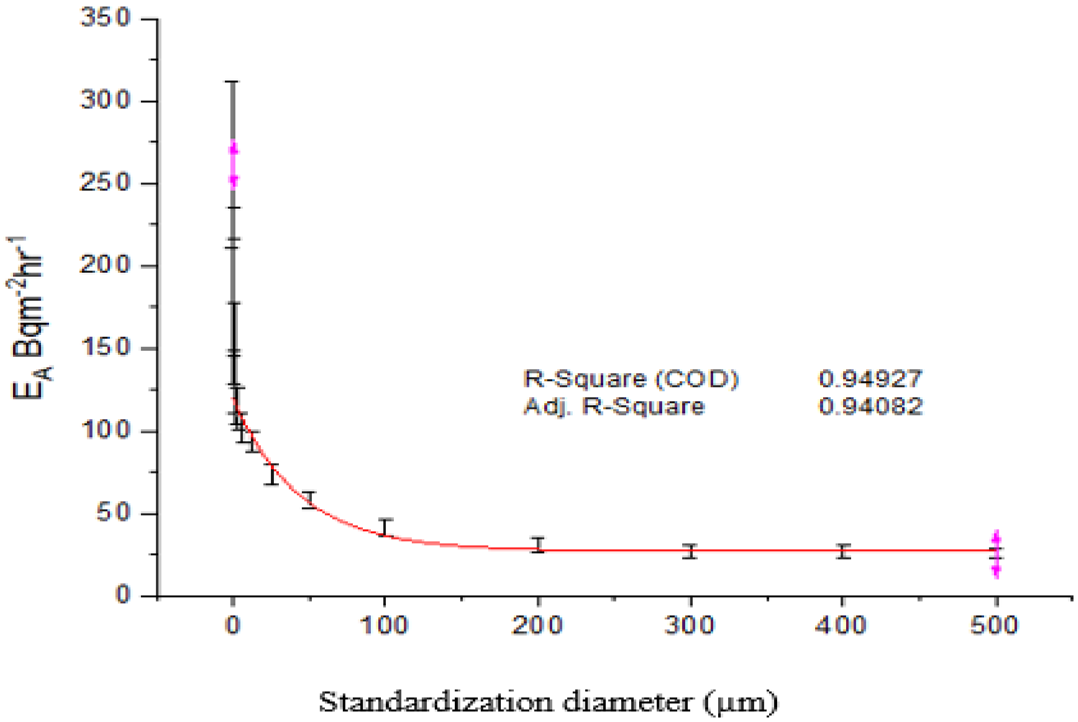

Fig. (9): Logarithmic correlation between E_A and standardization domain

Figures (8 and 9) prove the mentioned reverse proportion which strongly depends on the physical sample domain parameters and its frequency, rather wide spaces catalyze C_{Rn} and E_A diffuse respectively. Fig. (7) shows a significant exponential linkage between C_{Rn}, and E_A for the investigated samples. The linkage is exponential because the E_A equation hinges on C_{Rn} since the surface area of samples, volume of cans, and decay constant of radon gas are the same parameters for every sample [17, 36, 40-47].

The result of the present research project is compatible with the IAEA radiological survey that concerns radon concentration in dwellings [17, 36, 42], in addition to ICRP recommended the admissible threshold of radon concentration range (200 to 600) Bqm^{-3} [40, 41, 43].

CONCLUSION

The study is carried out to investigate the radiological impact of calcium silicate rocks which are used widely in building materials and other industrial proposes. The study explained the exponential relation between C_{Rn} and E_A which indicated the grain size domain is the most physical parameter that influence on radioactivity of radon and accesses quantification of its exhalation rate. Alpha track sheets LR-115 NTD is a good detector for monitoring radon concentration radioactivity and helps in the appreciation of possible radiological hazards. Regarding to exponential correlation relation between radon concentration and exhalation rate, cement material or other industrial products of infrastructures must be in the domain range (D10:D15) mentioned in Table (2) this is because to avoid and scale down of radon exhalation rate process from the building materials. The study's findings aid in recognizing any changes in the radioisotope background level caused by hydrothermal and geological processes related to the exploration and mining of calcium silicate ore.

ACKNOWLEDGMENT: The authors would like to thank the National Network for Nuclear Science in Egypt for the scientific collaboration through the Excellence Young Scientist Grant (NNS-EYSG).

Author contributions: A. Abdelrazek: Supervision, validation, conceptualization, methodology, writing—review; M. Mitwalli: Writing—original draft, editing, data curation, visualization, investigation, formal analysis, materials preparation.

Funding: No funding is provided for the current research paper.

Data availability: All data presented in this study are included in the article.

Declarations Competing interest: The authors declare that they have no known competing financial interests or personal relationships that could have appeared to influence the work reported in this paper.

REFERENCE

[1] Mitwalli, M., et al., *Environmental Radioactivity Monitoring Using High Resolution Gamma-ray Spectrometer for Lake Manzala in Egypt.* Arab Journal of Nuclear Sciences and Applications, 2022. **55**(4): p. 139-149.

[2] Ershaidat, N.M., B.A. Al-Bataina, and S.A. Al-Shereideh, *Characteristics of soil radon transport in different geological formations.* Environmental Geology, 2008. **55**(1): p. 29-35.

[3] Prati, C. and M.G. Gandolfi, *Calcium silicate bioactive cements: Biological perspectives and clinical applications.* Dental Materials, 2015. **31**(4): p. 351-370.

[4] Wang, P., et al., *Molecular dynamics simulation of the interfacial bonding properties between graphene oxide and calcium silicate hydrate.* Construction and Building Materials, 2020. **260**: p. 119927.

[5] Yu, Z., A. Zhou, and D. Lau, *Mesoscopic packing of disk-like building blocks in calcium silicate hydrate.* Scientific Reports, 2016. **6**(1): p. 36967.

[6] Shie, M.Y., H.C. Chang, and S.J. Ding, *Effects of altering the Si/Ca molar ratio of a calcium silicate cement on in vitro cell attachment.* International Endodontic Journal, 2012. **45**(4): p. 337-345.

[7] Dawood, A.E., et al., *Calcium silicate-based cements: composition, properties, and clinical applications.* Journal of Investigative and Clinical Dentistry, 2017. **8**(2): p. e12195.

[8] 8. Green, P.F., et al., *A study of bulk-etch rates and track-etch rates in CR39.* Nuclear Instruments and Methods in Physics Research, 1982. **203**(1): p. 551-559.

[9] Nikezic, D. and K.N. Yu, *Formation and growth of tracks in nuclear track materials.* Materials Science and Engineering: R: Reports, 2004. **46**(3): p. 51-123.

[10] Saleh, G.M., et al., *Environmental Radioactivity of Radon and its Hazards in Hamash Gold Mine, Egypt.* Arab Journal of Nuclear Sciences and Applications, 2019. **52**(4): p. 190-196.

[11] MITWALLI, M., et al., Evaluation of Radon Radioactivity and Radiological Impact by Using Solid-State Nuclear Track Detector for Erediya younger granites of Central Eastern Desert in Egypt. Arab Journal of Nuclear Sciences and Applications, 2023. **56**(3): p. 81-94.

[12] MITWALLI, M., et al., Radionuclides Determination and Computing Radiobiological Dose for TENORM Exposure Using NaI(Tl) Gamma-ray Spectrometer. Arab Journal of Nuclear Sciences and Applications, 2023. **56**(5): p. 114-126.

[13] MITWALLI, M., et al., *Radon Measurement and Radiological Dose Assessment From Terrestrial Rocks Using Solid-State Nuclear Track Detectors.* Arab Journal of Nuclear Sciences and Applications, 2022: p. 1-8.

[14] Ng, F.M.F., et al., *Non-destructive measurement of active-layer thickness of LR 115 SSNTD.* Radiation Measurements, 2004. **38**(1): p. 1-3.

[15] Tommasino, L., G. Zapparoli, and R. Griffith. *ELECTROCHEMICAL ETCHING–I MECHANISMS*. in *Solid State Nuclear Track Detectors: Proceedings of the 10th International Conference, Lyon, 2-6 July 1979*. 2013. Elsevier.

[16] El Ghazaly, M. and N.M. Hassan, *Characterization of saturation of CR-39 detector at high alpha-particle fluence.* Nuclear Engineering and Technology, 2018. **50**(3): p. 432-438.

[17] IAEA, *National and Regional Surveys of Radon Concentration in Dwellings*. 2014, Vienna: International Atomic Energy Agency.

[18] Iyer, R. and B.E. Lehnert, *Effects of ionizing radiation in targeted and nontargeted cells.* Archives of biochemistry and biophysics, 2000. **376**(1): p. 14-25.

[19] Musshoff, F., et al., *Two cases of suicide by asphyxiation due to helium and argon.* Forensic science international, 2012. **223**(1-3): p. e27-e30.

[20] Stanley, F.K., et al., *Comprehensive survey of household radon gas levels and risk factors in southern Alberta*. CMAJ open, 2017. **5**(1): p. E255.

[21] Simms, J.A., et al., *Younger North Americans are exposed to more radon gas due to occupancy biases*

within the residential built environment. Scientific reports, 2021. **11**(1): p. 1-10.

[22] Meenakshi, C., K. Sivasubramanian, and B. Venkatraman, *Nucleoplasmic bridges as a biomarker of DNA damage exposed to radon.* Mutation Research/Genetic Toxicology and Environmental Mutagenesis, 2017. **814**: p. 22-28.

[23] Hamza, V.Z. and M.N. Mohankumar, *Cytogenetic damage in human blood lymphocytes exposed in vitro to radon.* Mutation Research/Fundamental and Molecular Mechanisms of Mutagenesis, 2009. **661**(1-2): p. 1-9.

[24] Li, P., R. Zhang, and G. Zheng, *Genetic and physiological effects of the natural radioactive gas radon on the epiphytic plant Tillandsia brachycaulos.* Plant Physiology and Biochemistry, 2018. **132**: p. 385-390.

[25] Abu-Alam, T.S., K. Stüwe, and C. Hauzenberger, *Calc-silicates from Wadi Solaf region, Sinai, Egypt.* Journal of African Earth Sciences, 2010. **58**(3): p. 475-488.

[26] Abu-Alam, T. and K. Stüwe, *Exhumation during oblique transpression: the Feiran–Solaf region, Egypt.* Journal of Metamorphic Geology, 2009. **27**(6): p. 439-459.

[27] ISO, *International vocabulary of metrology - Basic and general concepts and associated terms*. 2007, International Organization for Standardization, ISO.

[28] ISO, *Uncertainty of meas-urement - Part 3: Guide to the expression of uncertainty in measurement ISO/IEC*, in *Supplement 1: Propagation of distribution us-ing the Monte Carlo method*. 2008, International Organization for Standardization

[29] Abbas, Y.M., et al., *Measurement of 226Ra concentration and radon exhalation rate in rock samples from Al-Qusair area using CR-39.* Journal of Radiation Research and Applied Sciences, 2020. **13**(1): p. 102-110.

[30] Yousef, H.A., et al., *Radon exhalation rate for phosphate rocks samples using alpha track detectors.* Journal of Radiation Research and Applied Sciences, 2016. **9**(1): p. 41-46.

[31] Singh, S. and S. Prasher, *The etching and structural studies of gamma irradiated induced effects in CR-39 plastic track recorder.* Nuclear Instruments and Methods in Physics Research Section B: Beam Interactions with Materials and Atoms, 2004. **222**(3): p. 518-524.

[32] Othman, S., et al., Investigation of radon concentration level and its progeny in different kinds of cancer by using Cr-39 NTD. Radiation Effects and Defects in Solids, 2023. **178**(3-4): p 456-484.

[33] Tripathi, R.M., et al., *Study of uranium isotopic composition in groundwater and deviation from secular equilibrium condition.* Journal of Radioanalytical and Nuclear Chemistry, 2013. **295**(2): p. 1195-1200.

[34] Todd, D.K. and L.W. Mays, *Groundwater hydrology*. 2004: John Wiley & Sons.

[35] Ivanovich, M., *Uranium series disequilibrium: applications to environmental problems*. 1982: Clarendon Press.

[36] IAEA, *Analytical Methodology for the Determination of Radium Isotopes in Environmental Samples*. 2011, Vienna: International Atomic Energy Agency.

[37] Shafi ur, R., et al., *Determination of 238U contents in ore samples using CR-39-based radon dosimeter—disequilibrium case.* Radiation Measurements, 2006. **41**(4): p. 471-476.

[38] Barooah, D. and P.P. Gogoi, *Study of radium content, radon exhalation rates and radiation doses in solid samples in coal-mining areas of Assam and Nagaland using LR-115 (II) nuclear track detectors*. 2019, India: Vishal Publishing Company.

[39] El-Farrash, A.H., H.A. Yousef, and A.F. Hafez, *Activity concentrations of 238U and 232Th in some soil and fertilizer samples using passive and active techniques.* Radiation Measurements, 2012. **47**(8): p. 644-648.

[40] UNSCEAR, *Sources and Effects of Ionizing Radiation*, ed. R.t.t.G. Assembly. Vol. 1. 2000, New York: United Nations Scientific Committee on the Effects of Atomic Radiation.

[41] UNSCEAR, *Report of the United Nations Scientific Committee on the Effects of Atomic Radiation* UNSCEAR, 2011. **58**: p. 12.

[42] IAEA, *Nuclear Data for the Production of Therapeutic Radionuclides*. 2012, Vienna: International Atomic Energy Agency.

[43] ICRP, *Protection Against Radon-222 at Home and at Work*. 1993, ICRP. p. . Ann. ICRP 23 (2).

[44] Harb, S., N. Ahmed, and S. Elnobi, *Effect of grain size on the radon exhalation rate and emanation coefficient of soil, phosphate and building material samples*. J Nucl Part Phys, 2016. **6**: p. 80-87.

[45] Pinto, P.V., K.S. Kumara, and N. Karunakara, *Mass exhalation rates, emanation coefficients and enrichment pattern of radon, thoron in various grain size fractions of monazite rich beach placers.* Radiation Measurements, 2020. **130**: p. 106220.

[46] Chitra, N., et al., *Study of radon and thoron exhalation from soil samples of different grain sizes.* Applied radiation and isotopes, 2018. **133**: p. 75-80.

[47] Ahmad, N., M.S. Jaafar, and S.A. Khan, *Correlation of radon exhalation rate with grain size of soil collected from Kedah, Malaysia.* Sci. Int, Lahore, 2014. **26**(2): p. 691-696.